19th Brazilian Congress of Thermal Sciences and Engineering
November 06th-10th, 2022, Bento Gonçalves - RS - Brazil

ENC-2022-0252
AN IMAGE-BASED TECHNIQUE FOR ICE QUALITY EVALUATION

Fabio de Souza Melo
Vitor Alexandre Massochin
Christian Johann Losso Hermes
POLO Labs, Departament of Mechanical Engineering, Federal University of Santa Catarina, Florianópolis, SC, Brazil
fabio.melo@polo.ufsc.br

Rodrigo Perito Cardoso
LabMat, Department of Mechanical Engineering, Federal University of Santa Catarina, Florianópolis, SC, Brazil

Abstract. *Due to the upcoming demand for ice that lasts longer and has a better appearance, clear ice has become a target for the refrigerator manufacturers. Although qualitative evaluations have been adopted over the years, particularly on industrial grounds, development of cutting-edge techniques for high-quality ice production relies on quantitative measurements, which are not only more accurate but also less subjective than the qualitative ones. Therefore, in this study, an image-based ice quality evaluation technique is proposed. A purpose-built apparatus was especially designed and constructed in such a way that a controlled environment and a professional camera are used to take pictures from the faces of a 125-cc ice cube. After this step, the images undergo a thresholding procedure, where the RGB matrix of the picture is transformed into grayscale and then binarized. Such an approach was able to identify the regions with flaws and, therefore, to calculate a figure of merit representative of the ice clearness, which is expressed by grades spanning from 0 (opaque) to 10 (translucent). Such a methodology was validated using ice cubes with distinct quality produced by means of another purpose-built apparatus that controls the freezing rate as well as the water agitation during ice making.*

Keywords: *Ice quality evaluation, Clear ice, Ice making, Image-based technique*

1. INTRODUCTION

The ice market, estimated to achieve a market value of US$5.9 billion dollars until 2023 (Imarc, 2018), is not focused only on the production rate, but also in the quality of ice. Some techniques were adopted in order to reduce the solidification rate and to reduce impurities or gases dissolved in the water that could affect the clarity of the ice. Unidirectional freezing in isolated containers without lid is an example of such techniques (Wondrich and Rothbaum, 2022).

This type of solidification is known as the Stefan Problem, since Josef Stefan was the first researcher to investigate this phenomenon while studying the growth of polar ice (Carslaw and Jaeger, 1959). The problem consists in freezing a bulk of water upwards and to calculate how the ice front growths, with a prescribed temperature on the base and adiabatic walls. The solution of the Stefan Problem, typical of diffusive problems, results in a solidification front position varying with the square root of time as described in Eq. (1):

$$z\,(t) = \sqrt{2\alpha_s Ste.\,t} \tag{1}$$

where z is the is the position of the interface regarding the origin of the coordinate system, α_s is the thermal diffusivity of the solid phase, t is time and Ste is the Stefan Number, a dimensionless parameter, described in Eq. (2), that represents the relative importance of the sensible heat in respect of the latent heat (Özisik, 1993).

$$Ste = \frac{c_p(T_f - T_c)}{h_{SL}} \tag{2}$$

where c_p is the specific heat at constant pressure, T_f is the solidification temperature, T_c is the temperature on the base of the container and h_{SL} is the latent heat of solidification. Despite Eq. (1) been the most common approach for Stefan Problems, another boundary condition can be considered. Besides prescribing temperature on the bottom surface,

prescribing heat flux is a possibility where the ice front advances linearly with time, as shown in Eq. (3), while the temperature on the base decreases accordingly to compensate the raise on global thermal resistance.

$$z\,(t) = \frac{q"}{\rho_s h_{SL}} t \tag{3}$$

where q" is the heat flux removed from the ice and ρ_s is the density of the solid phase.

The literature has lots of research on air bubbles inside the ice, which are responsible for the opacity usually seen in ice cubes (Carte, 1961). Studies done by Bari and Hallett (1974) about the nucleation and growth of bubbles at different freezing rates showed ranges of velocity where bubbles will be egg-shaped, cylinders or expelled, producing clear ice. However, this study did not compare the clarity of samples produced in distinct conditions.

Otherwise, Azuma et al. (2012) performed experiments regarding normal grain growth using polycrystalline ice samples. The normal grain growth is shown in Eq. (4).

$$D^n - {D_0}^n = kt \tag{4}$$

where D is the mean grain size at time t, D_0 is the mean grain size at t = 0, n is the grain growth exponent and k is a temperature-dependent constant. One of the results is that the exponent n varies between 5.3 and 14.5 for ice with air bubbles, while for clear ice, the exponent has less variation and is closer to the theoretical value of 2.

Although this result can be used as a quantitative parameter to evaluate the quality of ice, the experiments were not practical in terms of an assessment methodology, because they took long periods of time to be done and required visualization of the material microstructure with microscopes. Here, we present an image-base technique for evaluating ice quality with a cutting-edge procedure in order to quantify the clarity of ice samples.

2. METHODOLOGY

2.1 Experimental apparatus for ice production

The ice samples used to validate the methodology were produced in a test facility composed by an axial fan, a thermoelectric system, an ice tray and an insulating box. The concept of the apparatus enables to remove heat from the bottom of the tray and to vary the prescribed temperature as well as the prescribed heat flux. A heat flux transducer made with a copper plate is positioned underneath the tray to enhance the heat transfer to the refrigeration system. Figure 1 shows a scheme of the test facility used to produce the ice samples.

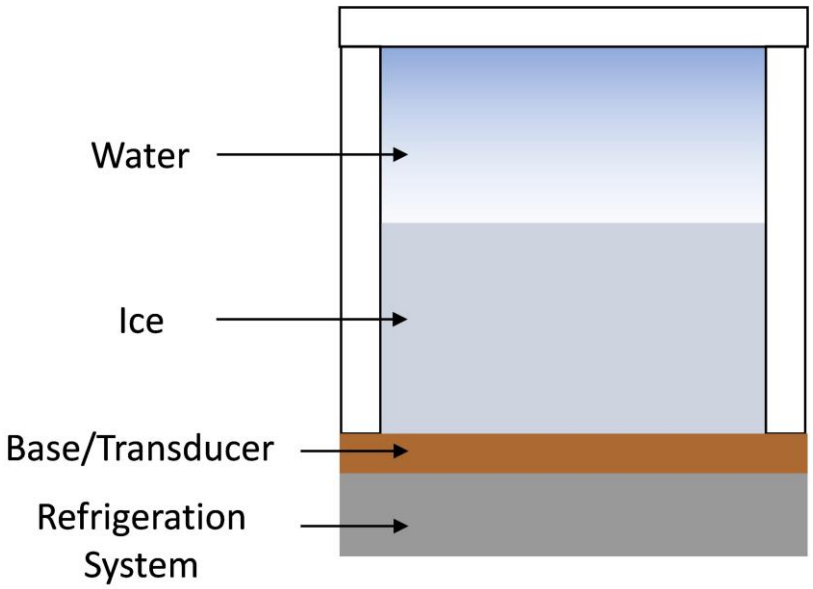

Figure 1. Scheme of the test facility for ice production.

The purpose-built apparatus was constructed using a Peltier module for the cooling system. This assembly was attached to a stepper motor to promote agitation on the water since Wilcox and Kuo (1973) have concluded that stirring decreases the tendency to form gas bubbles, which is the goal for clear ice production. Figure 2 shows the test facility for ice production coupled to the stepper motor.

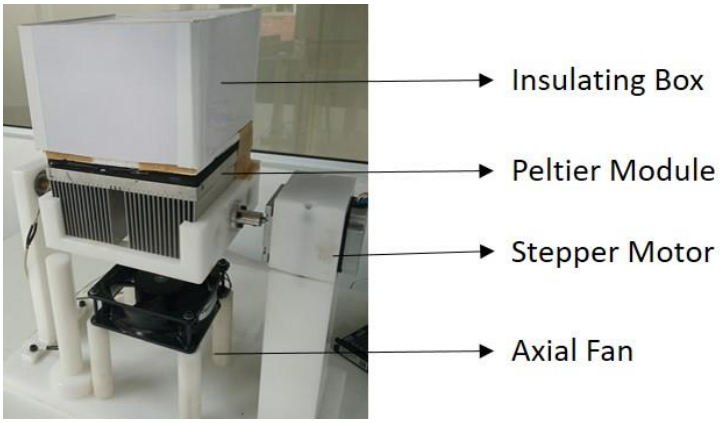

Figure 2. Test facility for ice production coupled to the stepper motor.

2.2 Experimental apparatus for ice quality evaluation

The ice quality evaluation technique proposed here is based on image capturing and processing. Since ice can be totally clear depending on the fabrication conditions, the photograph needs to be taken in a controlled environment in order to avoid light infiltration from the experimental room. Such apparatus was designed and built with black walls, a 6W-LED panel on the bottom, a black recipient with a transparent base, a professional camera and a black cloth covering the entire setup. The ice sample is submerged in cooled alcohol (-15°C) to avoid excessive melting during the procedure. The choice of using a black enclosure and illumination from the bottom has proven to be useful to highlight the borders of the ice samples.

The camera used for the image capture is a Cyber-shot DSC-HX300 in manual exposure mode to regulate and fix the adjustment parameters. These settings are ISO value 80, Shutter speed 250, Aperture value F8.0, Exposure Compensation 0EV. These features adjust the luminous sensitivity, the exposure time required for full closure of the shutter, the brightness of the image that passes through the lens and the compensation of the exposure before capture, respectively. Figure 3 presents a scheme of the purpose-built apparatus used to capture the images for ice quality evaluation.

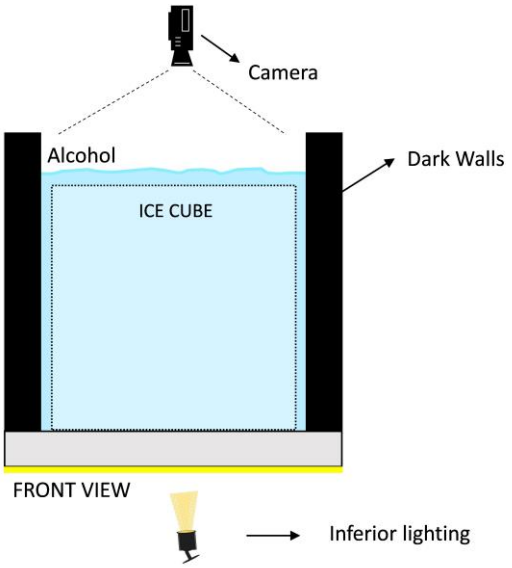

Figure 3. Scheme of the purpose-built apparatus used to capture the images for ice quality evaluation.

2.3 Image capturing and processing

This step of the method consists in positioning the ice cube in the center of the vessel. The cold alcohol helps to identify and highlight the ice borders. Figure 4 shows a picture of an ice sample inside the vessel with alcohol. After capturing pictures from the desired face of the ice cube, the images are transferred to a computer for the image processing with the Python OpenCV library.

Figure 4. Representative picture of an ice sample inside the vessel with alcohol.

For image processing, the first step is to calculate the total area of the ice face. In order to do so, only the ice is cropped from the picture and relocated in a green background (Fig. 5a). Then, the non-green pixels are summed to obtain the total area of ice. After that, the image is transformed into grayscale and binarized (Fig. 5b) using an automatic image thresholding called Otsu´s method, where an optimum threshold is selected based on the integration of the gray level histogram (Otsu, 1979).

At last, the image, with only black and white pixels, is used to count the pixels considered flaws in the structure, where the light was uncapable to pass through the ice. A similar image treatment to analyze gas bubbles has been used by Li et al. (2011) to measure the bubbles diameter and calculate their size distribution in a horizontal section of ice.

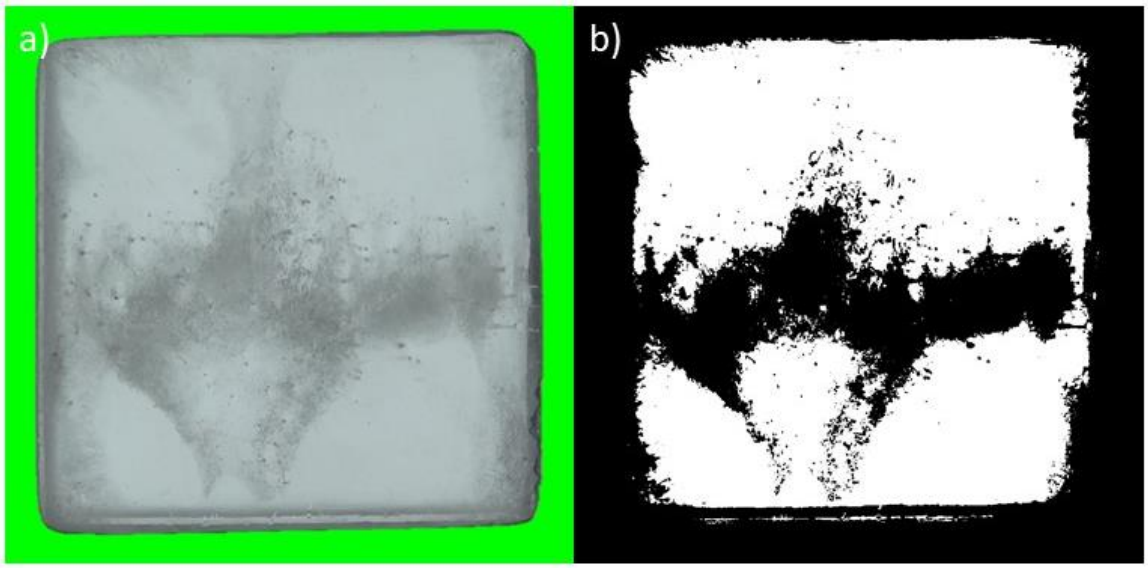

Figure 5. Representative picture of an ice image a) with the green background; b) after the thresholding procedure (Fig. 4 after image processing).

After counting the flaws pixels, a figure of merit is calculated based on the opaque area in relation to the total area of the sample. The result is expressed in grades varying between 0 to 10, where the minimum grade represents a completely opaque ice whereas the maximum represents a perfect clear ice sample. The ice cube face showed in Fig. 5b had a 6.1 grade, therefore, 61% of this face area is considered clear. In order to obtain a better representation of the entire cube, pictures of the other faces need to be taken and an average figure of merit is calculated.

3. RESULTS AND DISCUSSION

Three samples of ice were produced in different conditions. Pictures from all the sides were taken and each image were processed using the same methodology proposed in this work. The first test was done with a prescribed temperature of -12°C on the base and figures 6a, 6b, 6c, 6d, 6e and 6f shows the pictures taken inside the purpose-built apparatus, the ice production took 6h.

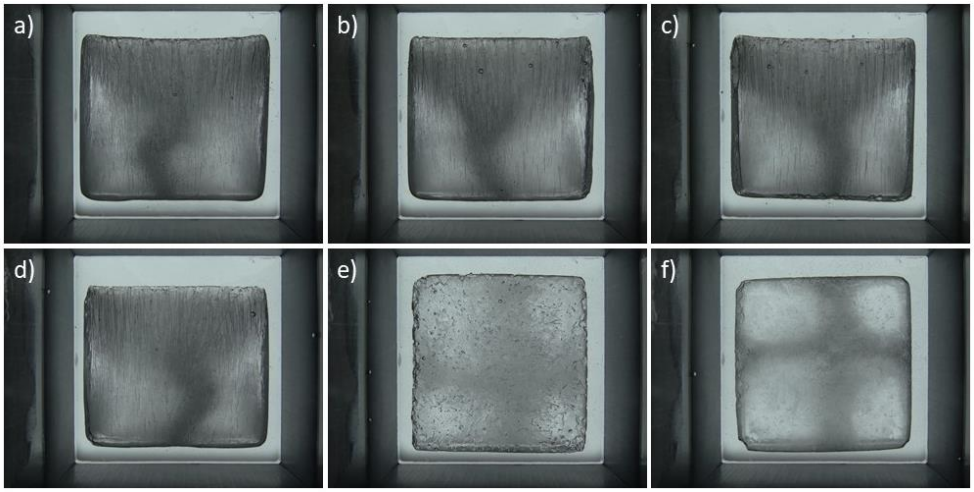

Figure 6. Test with -12°C and 6h production pictures of the a) front; b) right; c) back; d) left; e) top; f) bottom side taken inside the purpose-built apparatus.

It can be noticed that the bubbles trapped have a different aspect compared to the ice itself. Regions with a higher density of bubbles are darker and are easy to identify even without the threshold procedure. However, there are many bubbles with a cylindrical shape that does not appear clearly but avoids the passage of the light as well. Geguzin and Dzuba (1981) explained in their study that the gas bubbles become elongated cylinders when the growth rate of the bubble radius is equal to the velocity of the ice front. These elongated inclusions in the solid can occupy large lengths and appear as dark lines after the binarization. After image processing, the figure of merit of each face was calculated accordingly to the proposed method in order to obtain an average grade of ice quality. Figure 7 present the processed images of the first sample and their respective grades.

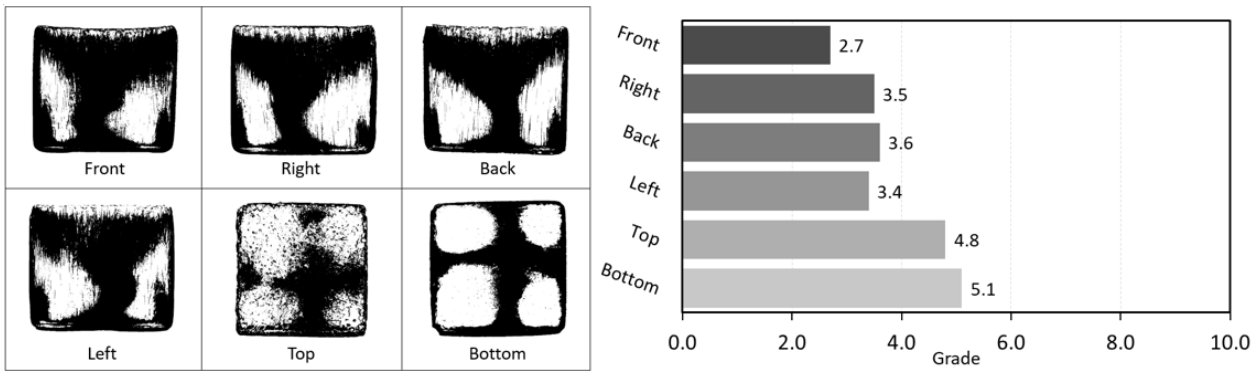

Figure 7. Processed images of the test with -12°C and 6h production and their respective grades.

The medium grade of ice sample showed in Fig 5 resulted in 3.8, or 38% of the total side area of the ice can be considered clear. It is visible that the top and bottom views had higher grades compared to the other areas. This can be explained by the fact that the extraction of heat from the water was in this direction and so bubbles are aligned in this direction. Therefore, the ice front was moving upwards and the trapped bubbles followed the moving interface during their elongation. So, the planes perpendicular to the direction of the ice growth had bubbles in the shape of dots instead of cylinders.

In the second ice sample, this pattern is more present due to the lesser ice growth rates during solidification. Also, it was done using the heat flux boundary condition, prescribing 500 W/m² to be removed from the bottom of the ice tray

(ice production took 12h). Figures 8a, 8b, 8c, 8d, 8e and 8f shows pictures taken for each ice face inside the purpose-built apparatus.

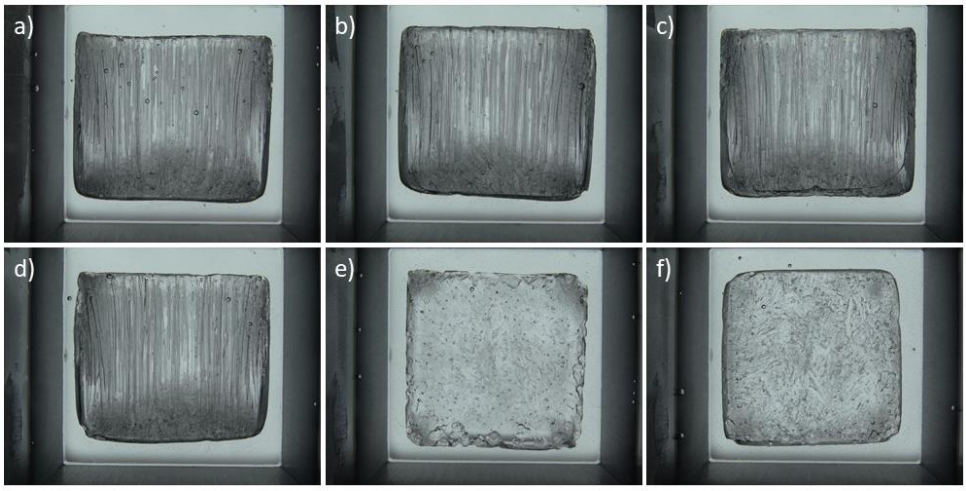

Figure 8. Test with 500 W/m² and 12h production pictures of the a) front; b) right; c) back; d) left; e) top; f) bottom side taken inside the purpose-built apparatus.

Comparing both ice samples, it can be spotted the difference of ice clarity by a simple visual analysis. The main idea of the methodology is to quantify this variation and avoid subjectivities. Applying the methodology proposed, the figure of merit of each ice cube side was calculated. Figure 9 present the processed images of the second sample and their respective grades.

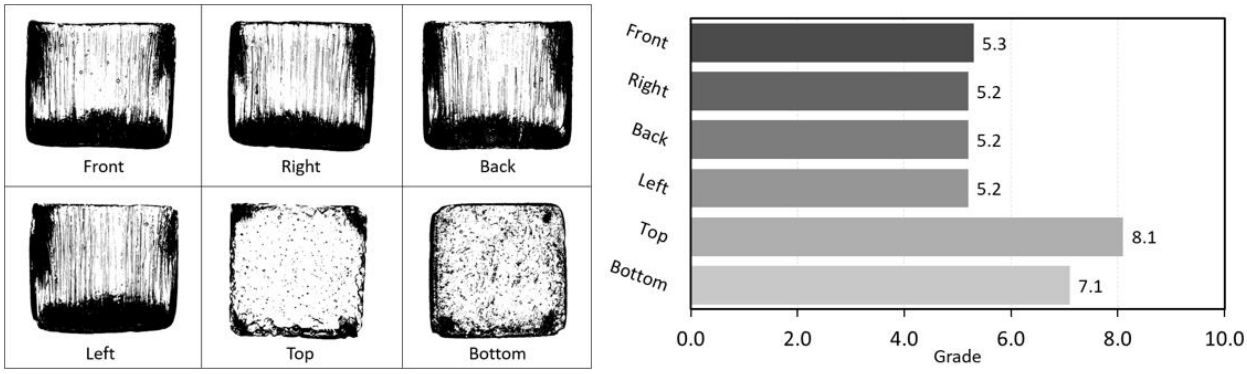

Figure 9. Processed images of the test with 500 W/m² and 12h production and their respective grades.

The medium grade of 6.0 was calculated and, following the same behavior as before, the top and the bottom faces had higher grades when compared to the sides. But in this second test, the dot shape of the bubbles can be easily seen on the top view, which did not happen on the bottom. These black marks that appears on the last view (bottom) are known as dendrites and are common in rapid solidification process where the phase change occur in temperatures below the freezing point (Bejan, 2006). The average grade of the second test was 2.2 points higher than the first test. This type of comparison is not possible using a qualitative evaluation methodology, given that the subjectivity of the evaluator has a strong influence in the final grade.

This distinction between grades happens due different solidification times. The velocity of the ice front is the throttle of this phenomenon, due to the built-up of an air supersaturation profile ahead of the moving interface. Tiller et al. (1953) explained this rejection of solute from the solid phase into the liquid phase during solidification of metals (in the case of water, air is the solute). Since the equilibrium concentration of solute in the solid is different from the liquid adjacent to it, it is possible to analyze the ratio of concentrations in both phases, which the literature calls it the distribution coefficient.

When this coefficient is lesser than 1 (for the water case, the order of magnitude is about 0.01), there is a progressively increase on the concentration of solute in the liquid near the solidification front. If the ice growth rate becomes higher, the development of the supersaturation condition follows the same behavior. When the concentration in the liquid reaches a critical value, bubbles may nucleate and get trapped in the ice if they do not have time to grow and scape by buoyancy.

Carte (1961) found in his experiments that this critical point of concentration is about 30 times higher than the initial saturated condition with air at 0°C.

After the nucleation, the bubble acts as a sink for the gas dissolved around its surface and reduces the concentration field during its growth. This process of buildup and depletion of the air supersaturation by the advance of the solidification front and nucleation and growth of bubbles, respectively, may occur periodically during the phase change. (Lipp et al., 1987).

The last test was done with the agitation system turned on and a prescribed temperature of -4°C (solidification took 20h). Even though the stirring improved the clarity of the sample, it still visible that dendritic solidification took place in the early stage of the process. Figures 10a, 10b, 10c, 10d, 10e and 10f shows the third sample pictures taken inside the purpose-built apparatus and figure 11 present the processed images of the third sample and their respective grades.

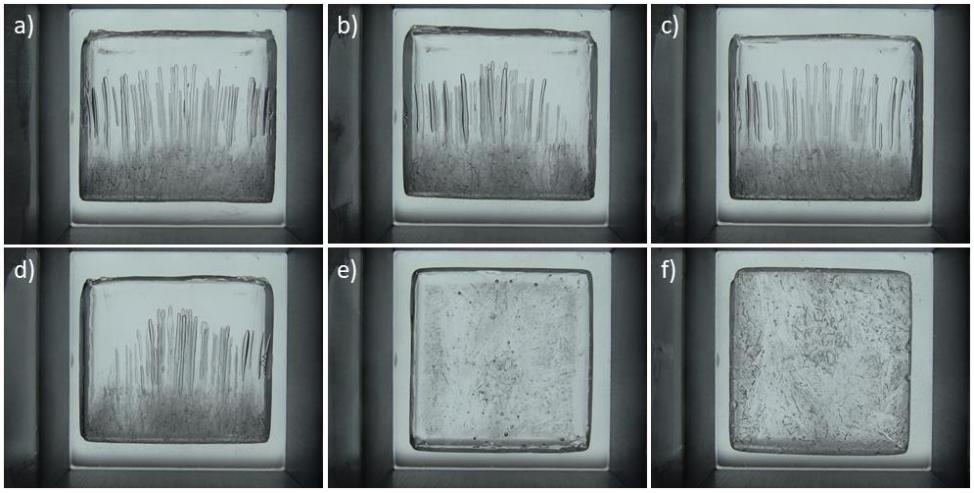

Figure 10. Test with -4°C and 20h production pictures of the a) front; b) right; c) back; d) left; e) top; f) bottom side taken inside the purpose-built apparatus.

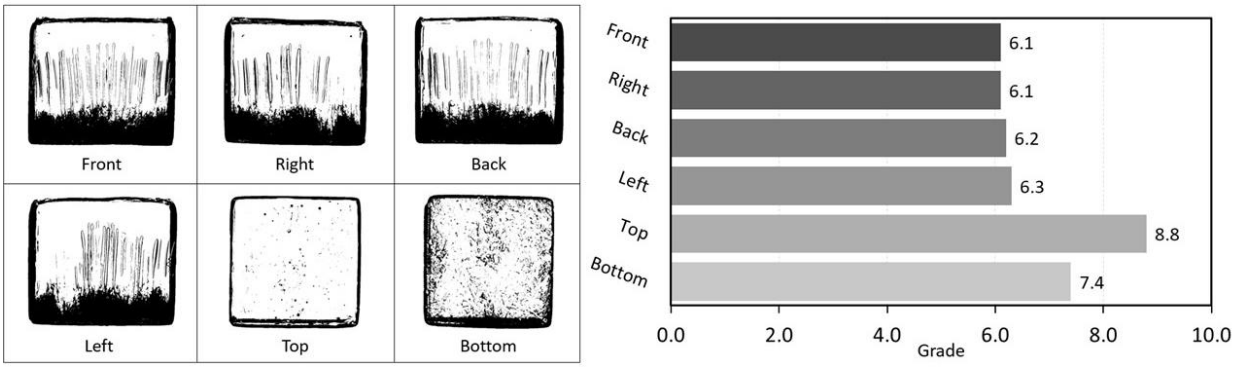

Figure 11. Processed images of the test with -4°C and 20h production and their respective grades.

As expected, the average grade was higher in this test when compared to the previous one due the agitation provided by the stepper motor. The grade of 6.8 was calculated and shows that this methodology can quantify the transparency of different ice samples, regardless of the method used to produce. Ice made in household refrigerators can be evaluated as well using this technique.

4. CONCLUSIONS

The image-based technique proposed in this work aims to assess the quality of different ice samples. This type of evaluation has a qualitative approach in industries grounds and the methodology developed avoids the subjectivity inherent to the evaluator. The method consists of capturing images in a controlled environment and image processing using the Python OpenCV library.

To compare different ice samples using the proposed technique and validate the method, 3 tests were done using distinct ice production conditions: the first with -12°C prescribed on the base of the ice tray, the second with 500 W/m² being removed from the base and the last, with -4°C prescribed on the base of the ice tray and the agitation system turned

on. The tests took 6h, 12h and 20h to be complete and the grades calculated were 3.8, 6.0 and 6.8, respectively. This grade represents the transparent area of the solid and is a quantitative parameter to compare the clarity of different samples. It is visible that slower freezing times increased the average grade of the ice, as well as the water agitation. The methodology proposed has proven to be useful for fundamental studies regarding ice formation and suits the necessity for quality evaluation in industrial grounds.

5. ACKNOWLEDGEMENTS

This work was carried out at POLO/UFSC under the auspices of the Institutos Nacionais de Ciência e Tecnologia program (CNPq 404023/2019-3, FAPESC 2019TR0846).

6. REFERENCES

Azuma, N. et al., 2012. "Impending Effect of Air Bubbles on Normal Grain Growth of Ice". *Journal of Structural Geology*. Vol. 42, pp. 184-193.

Bari, S. A., Hallett, J., 1974. "Nucleation and Growth of Bubbles at Ice-Water Interface". *Journal of Glaciology*, Vol. 13, No. 69, pp. 489-520.

Bejan, A., 2006. *Advanced Engineering Thermodynamics*. John Wiley & Sons, Inc., New Jersey, 3rd edition.

Carte, A. E., 1961. "Air Bubbles in Ice". *Proceedings of The Physical Society (1958-1967)*, Vol. 77, No. 3, pp. 757-768.

Carslaw, H. S., Jaeger, J. C., 1959. *Conduction of Heat in Solids*. Oxford University Press: London, 2nd edition.

Geguzin, Y. E., Dzuba, A. S., 1981. "Crystallization of A Gas-Saturated Melt". *Journal of Crystal Growth*, Vol. 52, p. 337-344.

Imarc, 2018. "Ice Maker Market: Global Industry Trends, Share, Size, Growth, Opportunity and Forecast 2018-2023". IMARC Group Archive, Report ID 4592317.

Li, Z. et al., 2011. "Distribution of Crystals and Gas Bubbles in Reservoir Ice during Growth Period". *Water Science and Engineering*, Vol. 4, No. 2, pp. 204-211.

Lipp, G. et al., 1987. "Investigation of The Behaviour of Dissolved Gases during Freezing". *Cryobiology*, Vol. 24, No. 6, pp. 489-503.

Otsu, N., 1979. "A Threshold Selection Method from Gray-Level Histograms". *IEEE Transactions on Systems, Man, and Cybernetics*, Vol. 9, No. 1, pp. 62-66.

Özisik, M. N., 1993. *Heat Conduction*. John Wiley & Sons, Inc., New York, 2nd edition.

Tiller, W. A. et al., 1953. "The Redistribution of Solute Atoms during The Solidification of Metals". *Acta Metallurgica*, Vol. 1, No. 4, pp. 428-437.

Wilcox, W. R., Kuo, V. H. S., 1973. "Gas Bubble Nucleation during Crystallization". *Journal of Crystal Growth*, Vol. 19, No. 4, pp. 221-228.

Wondrich, D., Rothbaum, N., 2022. *The Oxford Companion to Spirits and Cocktails*. Oxford University Press, New York, 1st edition.

7. RESPONSIBILITY NOTICE

The authors are the only responsible for the printed material included in this paper.